Polymer 50 (2009) 85–94

Contents lists available at ScienceDirect

Polymer

journal homepage: www.elsevier.com/locate/polymer

Structure–rheology relationships of long-chain branched polypropylene: Comparative analysis of acrylic and allylic coagent chemistry

J. Scott Parent [a,*], Aidan Bodsworth [a], Saurav S. Sengupta [a,b], Marianna Kontopoulou [a], Bharat I. Chaudhary [b], Drew Poche [c], Stéphane Cousteaux [c]

[a] Department of Chemical Engineering, Queen's University, Kingston, Ontario K7L 3N6, Canada
[b] The Dow Chemical Company, 171 River Road, Piscataway, NJ 08854, USA
[c] The Dow Chemical Company, Freeport, TX 77541, USA

ARTICLE INFO

Article history:
Received 12 August 2008
Received in revised form
1 November 2008
Accepted 6 November 2008
Available online 24 November 2008

Keywords:
Polypropylene
Long-chain branching
Rheology

ABSTRACT

The relationship between product structure and melt-state rheological properties is established for series of branched PP derivatives prepared by the radical-mediated grafting of tri-functional coagents. Peroxide-initiated, solvent-free additions of linear PP to triallyl trimesate (TAM), trimethylolpropane triacrylate (TMPTA) and triallyl phosphate (TAP) at high temperature are shown to produce bimodal molecular weight and branching distributions. Low-frequency dynamic shear viscosities as well as extensional viscosities are shown to be highly responsive to a hyper-branched chain population, whose abundance and molecular weight correlate with the kinetic chain length of the grafting process, and the propensity of a coagent to oligomerize.

1. Introduction

Long-chain branched polypropylene (LCB-PP) can provide the melt strength and extensional properties that are lacking in linear analogues [1–3]. As a result, methods of producing and characterizing these materials have attracted considerable interest [4–6]. A particularly attractive synthetic approach involves solvent-free reactive processing, wherein peroxide-initiated chain scission and coagent-assisted crosslinking transform the architecture of linear PP into branched materials. Indeed, several researchers have successfully combined the positive properties of solid state chemical modification with the production of a LCB-PP. Kim and Kim used the peroxide activation of four different coagents to produce LCB-PP samples whose melt rheological properties were characterized by melt flow index measurements [7]. Wang et al. extended this work to detailed analyses of the steady shear viscosity and molecular weight distribution of LCB-PP samples derived from reactions of PP with pentaerythritol triacrylate [8,9]. Analogous reaction products derived from trimethylolpropane triacrylate (TMPTA, Scheme 1) were prepared by Nam et al., who characterized melt-state rheological properties under oscillatory shear as well as extensional deformations [10]. Continuing on this line of research, Borsig et al. prepared LCB-PP materials using divinylbenzene, hydroquinone, and difurfuryl sulfide as coagents, and characterized these derivatives by single-detector GPC and oscillatory shear rheometry [11].

All of the aforementioned reports provide clear evidence of the generation of long-chain branching from linear PP parent materials, and document the influence of this branching on melt-state rheological properties. Our recent work has revealed the chemistry of triallyl trimesate (TAM, Scheme 1) grafting to PP, as well as the architecture of PP-*g*-TAM products [12]. At the temperatures and reagent loadings that are relevant to reactive extrusion, the graft modification of PP with TAM generates bimodal molecular weight and branching distributions. The extent to which the chain populations diverge is a function of the degree of simultaneous polymer fragmentation and crosslinking. Cleavage of linear chains yields low-mass fragments that are statistically less susceptible to coagent-induced crosslinking. On the other hand, fragmentation of high mass, branched structures has little impact on their molecular weight. As a result, extensive graft modification of PP with TAM yields a dominant chain population that is both degraded and slightly branched, and a minor, hyper-branched chain population whose molecular weight can extend beyond the gel point.

While the relative simplicity of TAM grafting chemistry makes it well suited to fundamental studies of graft structure, researchers have preferred acrylate-based coagents such as trimethylolpropane triacrylate (TMPTA, Scheme 1) [7,8]. This work sought to reveal the molecular weight and branching distributions generated by TAM,

* Corresponding author. Tel.: +1 613 533 6266; fax: +1 613 533 6637.
E-mail address: parent@chee.queensu.ca (J.S. Parent).

0032-3861/$ – see front matter © 2008 Elsevier Ltd. All rights reserved.
doi:10.1016/j.polymer.2008.11.014

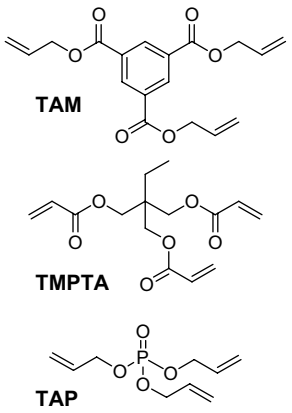

Scheme 1.

TMPTA, and triallyl phosphate (TAP, Scheme 1), and to relate product architecture to melt state rheological properties under oscillatory shear and extensional deformations. A secondary goal was to compare and contrast the kinetic reactivity and crosslinking efficiency of each coagent to define the range of branched PP architecture supported by this synthetic method.

2. Experimental

2.1. Materials

A metallocene-catalyzed ethylene–octene copolymer (PE, octene content = 7.3 mol%, MFI = 1.6 g/10 min, DuPont-Dow Elastomers) was used as-received. Samples destined for GPC studies were conducted with an additive-free grade of isotactic polypropylene homopolymer (LMW-PP, M_n = 43 kg/mol, polydispersity = 7.0, Dow Chemical). Samples destined for rheological studies were conducted from an additive free grade of isotactic polypropylene homopolymer (PP, M_n = 70.7 kg/mol, polydispersity = 5.5, Dow Chemical) that was used in powdered form without purification. Triallyl trimesate (TAM, Monomer Polymer Inc), triallyl phosphate (TAP, 98%, TCI), trimethylolpropane triacrylate (TMPTA, tech grade, Sigma–Aldrich) and 2,5-dimethyl-2,5-di(*t*-butylperoxy)hex-3-yne (L-130, Atofina) were used as-received.

2.2. Modification of PE

PE (40 g) was mixed with L-130 (0.08 g) and the desired amount of coagent at 100 °C using a Haake Polylab R600 internal batch mixer. An aliquot of the resulting masterbatch (5 g) was reacted in the cavity of an Alpha Technologies Advanced Polymer Analyzer at 200 °C using an oscillation arc of 3° and a frequency of 100 cpm. On-line measurements of dynamic storage (G') and loss (G'') moduli provided the information needed to report the rate of G' evolution with time as well as changes to complex viscosity.

2.3. Modification of PP

Powdered PP (3 g) was coated with a hexanes solution (8 ml) containing the desired quantity of L-130 and coagent. The hexanes were evaporated and the resulting mixture was charged to the preheated cavity of an Atlas Laboratory Mixing Molder at 200 °C for 6 min. The polymer product was pressed into thin sheets at 170 °C and mixed with a masterbatch of calcium stearate (500 ppm), Irganox 1010 (500 ppm) and Irgafos 168 (1000 ppm) by repeated folding and pressing.

Residual monomer contents were measured from xylene extracts using ^{1}H NMR spectrum integration of C=C content against an internal standard. Gel contents were determined by extracting material (0.5 g) from 120 mesh sieve cloth with refluxing xylenes (40 ml, stabilized with 1000 ppm butylated hydroxytoluene, BHT) for 6 h, with longer extraction times having no effect on the results. The residue was dried under vacuum to constant weight, with the yield of insoluble gel reported as the weight percent of the crude sample mass.

2.4. Analysis

NMR spectra were recorded with a Bruker AM-600 spectrometer in $CDCl_3$. Extensional viscosity measurements for PP samples were acquired at 180 °C using an SER Universal Testing Platform from Xpansion Instruments, which records the tensile stress growth coefficient as a function of time at different strain rates. The evolution of storage modulus (G') with time for polyethylene samples were measured with an Alpha Technologies Advanced Polymer Analyzer 2000 equipped with biconical dies at a frequency of 6.3 rad/s and a fixed strain of 4%. Oscillatory elastic (G') and loss (G'') moduli of polypropylene samples were measured under a nitrogen atmosphere using a Reologica ViscoTech controlled stress rheometer equipped with 20 mm diameter parallel plates. The instrument was operated at 180 °C with a gap of 1.5 mm over frequencies 0.04–188 rad/s. Stress sweeps were performed to ensure that all data were acquired within linear viscoelastic conditions. Creep and creep-recovery experiments were performed using the aforementioned instrument at 180 °C using a stress of 10 Pa, unless stated otherwise. Discrete relaxation spectra were constructed by fitting $G'(\omega)$ and $G''(\omega)$ measurements to the following equations [13]:

$$G'(\omega) = \sum_{i=1}^{N} g_i \frac{(\omega\lambda_i)^2}{1+(\omega\lambda_i)^2}$$

$$G''(\omega) = \sum_{i=1}^{N} g_i \frac{\omega\lambda_i}{1+(\omega\lambda_i)^2}$$

where λ_i is the relaxation time for element i, and g_i is its modulus. Values for g_i and λ_i were derived with a nonlinear optimization program employing the algorithm developed by Baumgartel and Winter [13]. This method estimates the least number of parameters (Parsimonious spectra) needed to obtain an adequate fit of the experimental data. The number of relaxation modes and the distribution of the relaxation times depend on the optimization of the simultaneous solution of the G' and G'' equations listed above.

Relaxation spectrum index (RSI) values were calculated from the ratio of the second and first moments of discrete time distribution [14,15] according to:

$$\mathrm{RSI} = \lambda_{\mathrm{II}}/\lambda_{\mathrm{I}}$$

where the first and second moments of the relaxation time distribution are, respectively:

$$\lambda_{\mathrm{I}} = \frac{\sum_i g_i}{\sum_i g_i/\lambda_i}$$

$$\lambda_{\mathrm{II}} = \frac{\sum_i g_i\lambda_i}{\sum_i g_i}$$

High temperature triple detection GPC analysis of *i*-PP and its derivatives was conducted in 1,2,4-trichlorobenzene (TCB) at 160 °C and 1 ml/min using a Polymer Labs PL 220 instrument

equipped with a Precision Detectors (Model 2040) light scattering instrument, for which the 15° angle detector was used for calculation purposes. The viscometer was a Viscotek model 210R detector. The column bank consisted of four 7.8 × 300 mm PL gel 20 micron Mixed A beds. The dn/dc value used for calculating molecular weights from the light scattering data was 0.104 mL/g. The detector responses were calibrated using an internally validated polyethylene standard. The samples were dissolved in BHT-stabilized TCB at 160 °C for approximately 2.5 h prior to analysis.

3. Results

Coagent-assisted PP modifications involve simultaneous chain scission and crosslinking. As noted above, the architectures generated by this process are quite complex, making it difficult to draw unambiguous conclusions regarding the kinetic reactivity and crosslinking efficiency of a given coagent. Therefore, our analysis of TAM, TMPTA and TAP began with studies of PE crosslinking dynamics and yields, before progressing to the more complex PP homopolymer system.

3.1. Coagent-assisted crosslinking of PE

Radical-mediated modifications of ethylene-rich polyolefins do not suffer from large-scale chain scission when conducted below 220 °C [16]. The dominant molecular weight altering reaction in the absence of a coagent is radical–radical combination, whose extent can be monitored up to and beyond the gel point by oscillatory shear rheometry. Fig. 1 illustrates the evolution of complex viscosity (η^*) with time for a series of L-130 initiated, PE crosslinking reactions. For the coagent-free formulation, η^* progressed from an initial value of 2.5 kPa s to a stable plateau of 8.0 kPa s after 7 min. Crosslinking dynamics paralleled those of initiator decomposition, since peroxide homolysis is the rate-determining step that supports radical–radical combination.

The inclusion of 3 wt% TAM (90 μmol/g) raised the η^* plateau substantially (Fig. 1), because repeated polymer addition to the C=C functionality of a coagent introduces a chain character to the crosslinking process. Whereas the number of crosslinks generated by a coagent-free cure cannot exceed one-half of the number of alkyl macroradicals initiated by the peroxide, TAM-graft additions can crosslink the polymer without reducing radical populations. This is true for all the coagents of interest, meaning that their effectiveness is dictated by two main factors. The first is kinetic chain length, which is defined as the number of coagent C=C bonds consumed by polymer addition over an average radical lifetime. It establishes the maximum number of crosslinks that can be produced from a given coagent + peroxide loading, and is expected to be a function of reagent concentrations, temperature, and the reactivity of a particular polymer–coagent pair with respect to C–H bond addition. The second factor is the propensity of a coagent toward homopolymerization, since this process consumes C=C bonds without contributing to crosslink density. An ideal coagent grafts to full C=C conversion, without engaging in oligomerization or cyclization.

The data presented in Fig. 1 illustrate the remarkable reactivity of TMPTA, as well as the pronounced improvements in crosslink density that can be gained from its use. The maximum rate at which the storage modulus increased (dG'/dt: kPa/min, Fig. 1) was 190 kPa/min for the TMPTA-assisted sample, compared to just 21 kPa/min for the coagent-free reaction. However, the rate of G' growth produced by TMPTA converged with that of TAM after just 30 s. This likely corresponds to the point of complete consumption of free TMPTA, after which network growth results mainly from radical–radical combination, along with the consumption of residual, polymer-bound acrylate functionality.

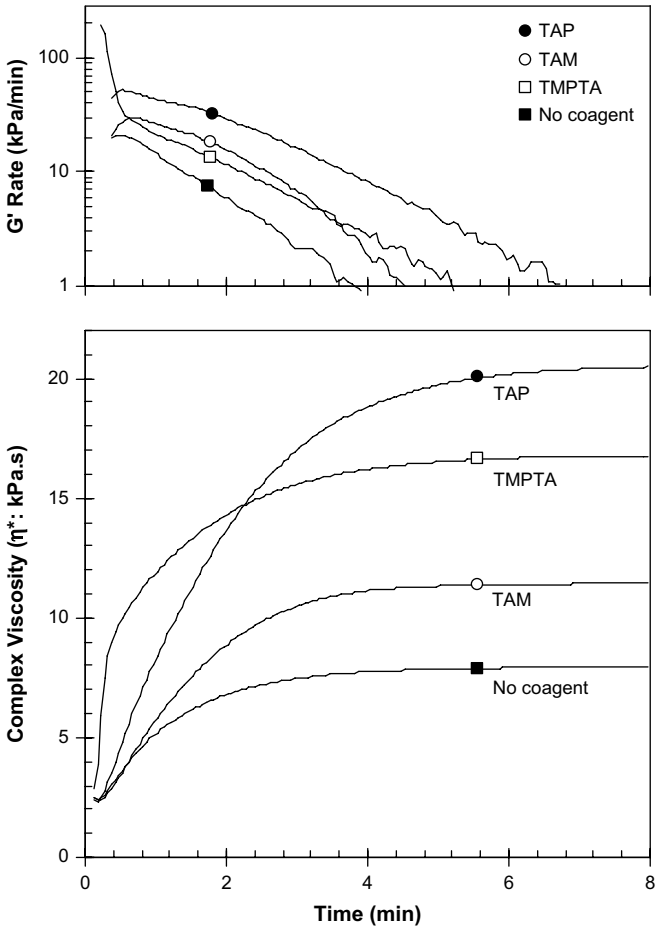

Fig. 1. Coagent-assisted peroxide cures of PE (200 °C; frequency = 6.3 rad/s; 0.2 wt% L-130 peroxide; 90 μmol/g coagent).

That TMPTA was consumed quickly is not surprising, given the exceptional reactivity of acrylates with respect to radical addition. The rate constant for ethyl acrylate homopolymerization is $k_p = 800\ M^{-1}\ s^{-1}$ at 50° [17], while the chain transfer constant to cyclohexane is $k_{tr}/k_p = 4.8 \times 10^{-5}$ in this temperature range [18]. This suggests that TMPTA is prone oligomerization. Indeed, the addition of mono-functional acrylates to polyolefins at high temperature has been shown to be a relatively inefficient process, leading to substantial amounts of homopolymer as well as long, oligomeric grafts [19].

Perspective on the crosslinking efficiency of TMPTA is provided by the corresponding data for the TAP system. The η^* versus time profile illustrated in Fig. 1 shows that TAP is not as kinetically reactive as the acrylate system, but it is capable of generating higher crosslink densities when given a sufficient amount of initiator. The potential of allylic systems to provide superior crosslinking yields stems from a lesser tendency to homopolymerize [20]. With less coagent consumed by oligomerization and, presumably, intramolecular cyclization, a fully converted allylic coagent will generate more crosslinks than a corresponding acrylate-based compound. Indeed, both TAM and TAP produced η^* plateaus about 1.3 times that of TMPTA when activated by 0.5 wt% of L-130 (not shown).

4. Structure of coagent-modified PP

The PE data described above has revealed patterns of kinetic reactivity (TMPTA ≫ TAP > TAM) and crosslinking potential (TAP ≅ TAM > TMPTA) for polyolefin modifications that are not dominated by macro-radical fragmentation. However, the

development of long-chain branching within PP involves simultaneous chain scission and coagent-assisted crosslinking, with the yield and selectivity of each reaction controlling the product architecture. Table 1 presents the structural data needed to interpret the melt-state rheology of coagent-modified PP.

The starting material for this GPC study was an unstabilized PP homopolymer (hereafter referred to as LMW-PP) with an M_n of 43 kg/mol and a polydispersity of 7.0. Its linear architecture is evident from the molecular weight distribution and intrinsic viscosity plots illustrated in Fig. 2. Treatment of this resin with 0.05 wt% of L-130 at 200 °C dropped its M_n by 37%, and reduced its polydispersity by half (Table 1). This is consistent with "controlled PP degradation" principles, where the highest molecular weight chains are statistically more likely to undergo radical-mediated scission [21].

We found that the reactivity and yield patterns established for the PE system applied equally well to coagent modifications of PP. Coagent conversions ranged from quantitative for TMPTA, to intermediate for TAP, and marginal for TAM (Table 1). Both TMTPA and TAP provided crosslinking yields that were sufficient to bring 4–5 wt% of LMW-PP beyond the gel point, while TAM failed to produce an isolable amount of hyper-branched gel under identical reaction conditions.

The molecular weight distribution data summarized in Table 1 show that chain scission dominated for all three coagent systems, since M_n values recorded for the majority chain populations were lower than those of the parent material. The GPC data illustrated in Fig. 2 for the TMPTA derivative is typical of a coagent-modified PP product. The matrix is substantially lower in molecular weight than the starting polymer, and it is accompanied by a minor, high molecular weight, chain population. The branched architecture of the latter material is evidenced by the intrinsic viscosity plot, which shows substantial negative deviation from the linear parent polymer at high molar mass. Note that this sample also contained 5 wt% of insoluble gel that is not represented by GPC analysis.

Based on these results, we can state with confidence that bimodality is an inherent characteristic not only of high temperature TAM-grafting reactions [12], but of TMPTA and TAP-based modifications as well. It is likely that bimodality is inherent to all polymerizable coagent-based processes, including the triacrylate system analyzed by Wang [9], and the divinylbenzene process studied by Borsig et al. [11]. Indeed, the solution viscometer response of Wang's GPC analyses shows some evidence of branch concentration amongst high molecular weight chains. While Borsig et al. [11] do not provide the Mark–Houwink plots that are needed to identify bimodal branching distributions, their divinylbenzene-based products contained gel and a soluble matrix whose molecular weight was below that of the parent material. This is consistent with a bimodal molecular weight distribution.

5. Rheology of coagent-modified PP

The stated objectives of this work were to further understand the structure–rheology relationships of this class of materials, and to define the scope of application for TAM, TMPTA and TAP. To this end, we have prepared a series of PP derivatives from a high molecular weight PP homopolymer ($M_n = 70.7$ kg/mol) using two concentrations of peroxide (0.05, 0.20 wt%) and coagent (45, 90 μmol/g PP). The melt-state rheology of these samples was evaluated under shear using creep and dynamic oscillatory measurements, and under elongation by monitoring extensional viscosity. These data provided the basis for estimating zero-shear viscosities (η_0), complex viscosities (η^*), discrete relaxation spectra, and the ratio of relaxation spectrum distribution moments, known as the relaxation spectrum index (RSI) [14]. Each coagent is described in turn, following a brief description of the base PP material and its peroxide-degraded derivatives.

Table 1
Properties of LMW-PP and its derivatives.[a]

Coagent	Coagent Conversion (%)	Gel Content (wt%)	M_n[b] (kg/mol)	M_n/M_w[b]
Unmodified	–	0	43	7.0
None	–	0	27	3.6
TAM	36	0	24	5.4
TMPTA	100	5	26	7.7
TAP	73	4	30	5.2

[a] [L-130] = 0.05 wt%; [Coagent] = 90 μmol/g; $T = 200$ °C; 6 min.
[b] Soluble component of reaction product.

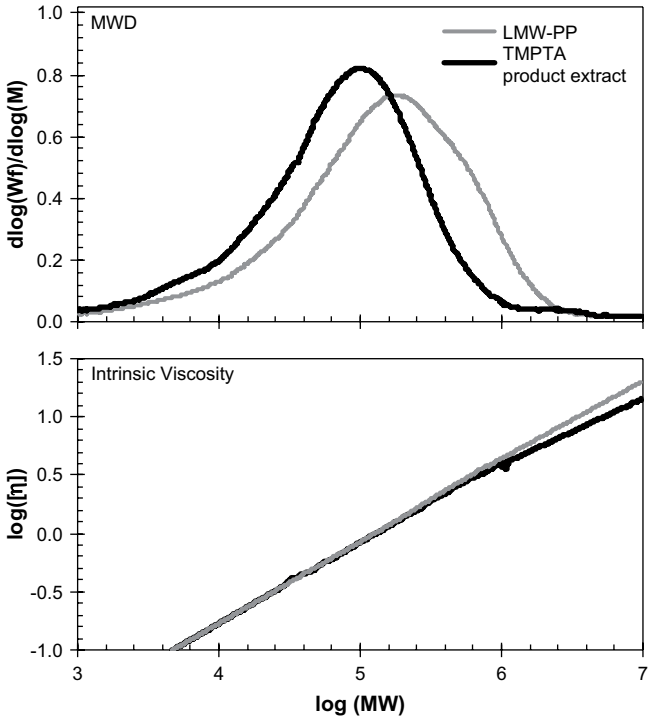

Fig. 2. GPC analysis of LMW-PP and the xylene-soluble component of its TMPTA-derivative (Table 1).

The linear structure of the parent material and its fragmented derivatives is reflected in their melt-state rheological properties (Fig. 3). Each material exhibited a Newtonian plateau, with the onset of shear thinning shifted to higher frequency as the extent of polymer fragmentation was increased, due in part to a reduction in polydispersity [22]. This narrowing of the molecular weight distribution was reflected in the relaxation time spectrum, whose relaxation spectrum index declined from 8.8 to a low of 1.1 under the most severe reaction conditions. No extensional strain hardening was observed, as PP and its mildly degraded analogue abided by Trouton's Law throughout the measurement.

A series of TAM-grafted products were prepared and analyzed to generate the data presented in Fig. 4. The reagent loadings used in this study did not produce an isolable amount of gel, and none of the product viscosities (η_0 and η^*) approached those of the starting material. Branching effects were most evident when reagent loadings were maximized (0.20 wt% L-130, 3.0 wt% TAM). This PP-*g*-TAM sample did not exhibit a Newtonian plateau over the frequency range studied, as the storage modulus failed to reach a terminal condition where G' scales with ω^2. Lower slopes for G' in this region have been documented by Nam et al. [10] and Borsig et al. [11], who attributed this behaviour to the influence of long-chain branching. Further insight is gained from a plot of tan δ versus

Symbol	[L-130] wt%	RSI	η_o Pa.s
□	---	8.8	11520
○	0.05	1.8	603
◇	0.20	1.1	82

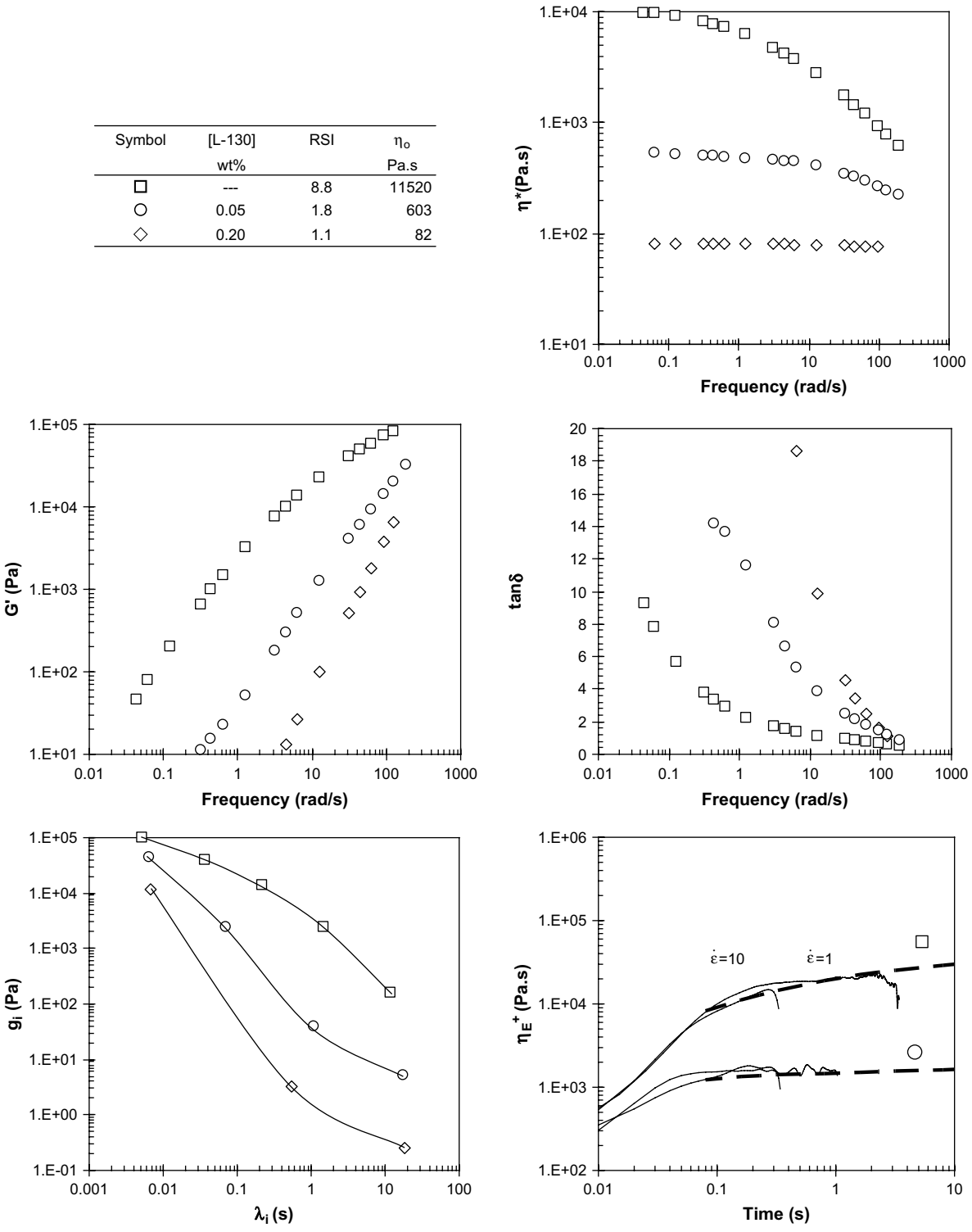

Fig. 3. Rheological data for PP and its degraded derivatives ($T = 180\,^{\circ}C$).

frequency, which reveals heightened elasticity at the low frequency range where branch entanglement effects are most pronounced [23,24]. As expected from a slightly branched PP derivative of low molecular weight, extensional strain hardening was minimal.

TMPTA produced more significant changes to the shear and extensional rheology of PP. Fig. 5 shows that, irrespective of the reaction conditions used, TMPTA grafting generated isolable gel fractions and pronounced extensional strain hardening characteristics. Discrete relaxation spectra contained elements with characteristic times exceeding 30 s, which were most pronounced when just 0.05 wt% of L-130 was used in conjunction with 2.3 wt% of TMPTA. Storage modulus (G') values were less sensitive at low frequencies when compared to the TAM system, and loss tangent data provide clear evidence of heightened elasticity in this frequency range. When compared to TAM, the data show TMPTA to be uniquely capable of generating hyper-branched material from very low initiator loadings. Since PP scission is also dependent on macro-radical concentrations, TMPTA supports

Symbol	[L-130] wt%	[TAM] wt%	RSI	η_o Pa·s	[Gel] wt%
○	0.05	1.5	3.8	1820	0
●	0.05	3.0	3.0	2660	0
◇	0.20	1.5	1.5	170	0
◆	0.20	3.0	2.5	960	0

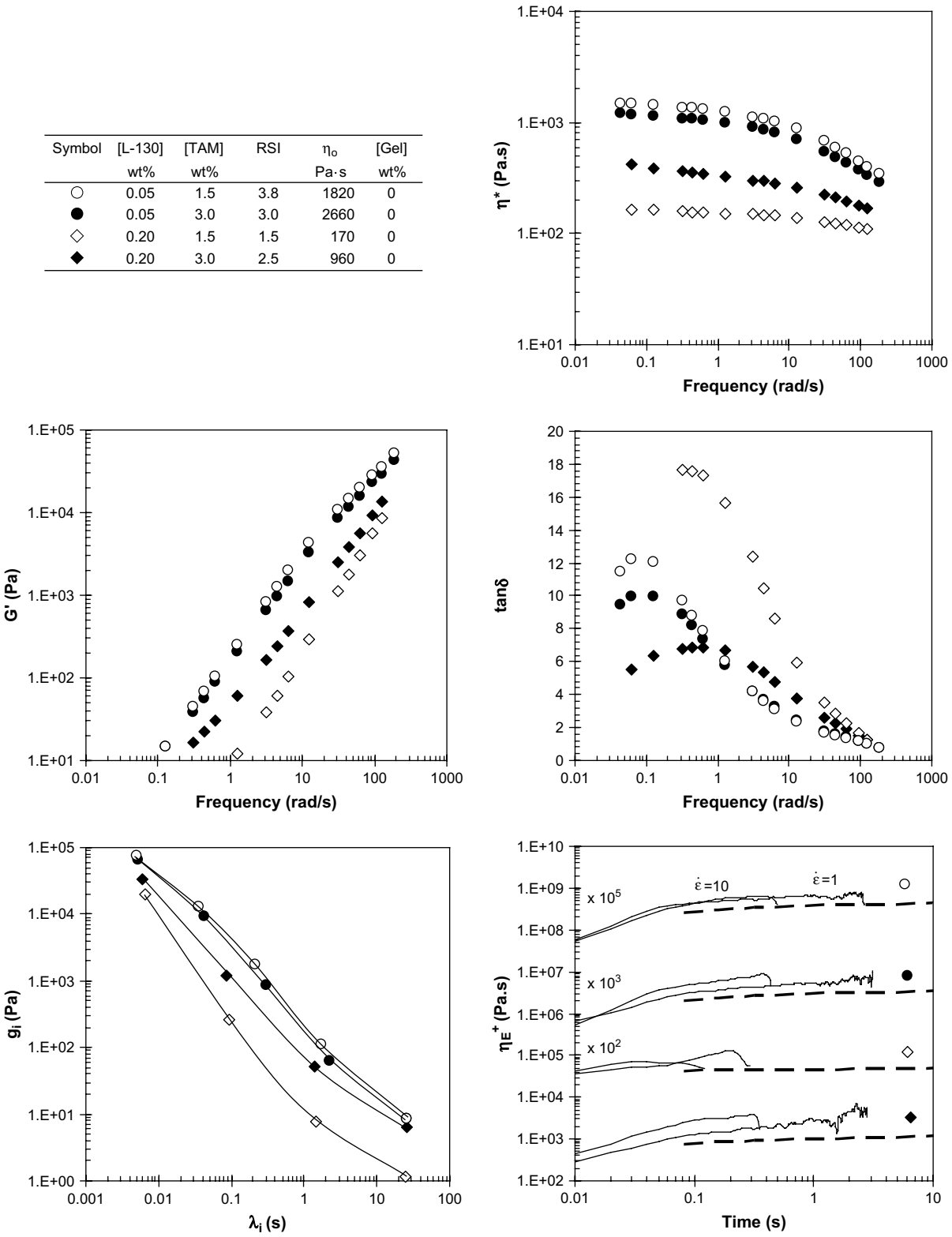

Fig. 4. Rheological data for PP-*g*-TAM products ($T = 180\ ^\circ C$).

a fragmentation/crosslinking balance that is distinct amongst the coagents studied in this work. This issue will be addressed further after a brief examination of the TAP system.

That TAP is kinetically less reactive than TMPTA, but more efficient in terms of crosslinking yield, is confirmed by the rheological data presented in Fig. 6. At low L-130 loadings, branching effects were only evident when a high TAP concentration was used to produce the requisite crosslink density and gel population. When activated by a high initiator loading, 3 wt% of TAP produced a remarkable gel content, which proved to be highly influential on low frequency shear properties and extensional strain hardening. The long relaxation time of this component is revealed by the

Symbol	[L-130] wt%	[TMPTA] wt%	RSI	η_o Pa·s	[Gel] wt%
○	0.05	1.3	5.2	4950	2
●	0.05	2.7	8.5	10500	5
◇	0.20	1.3	2.5	580	1
◆	0.20	2.7	4.8	1850	3

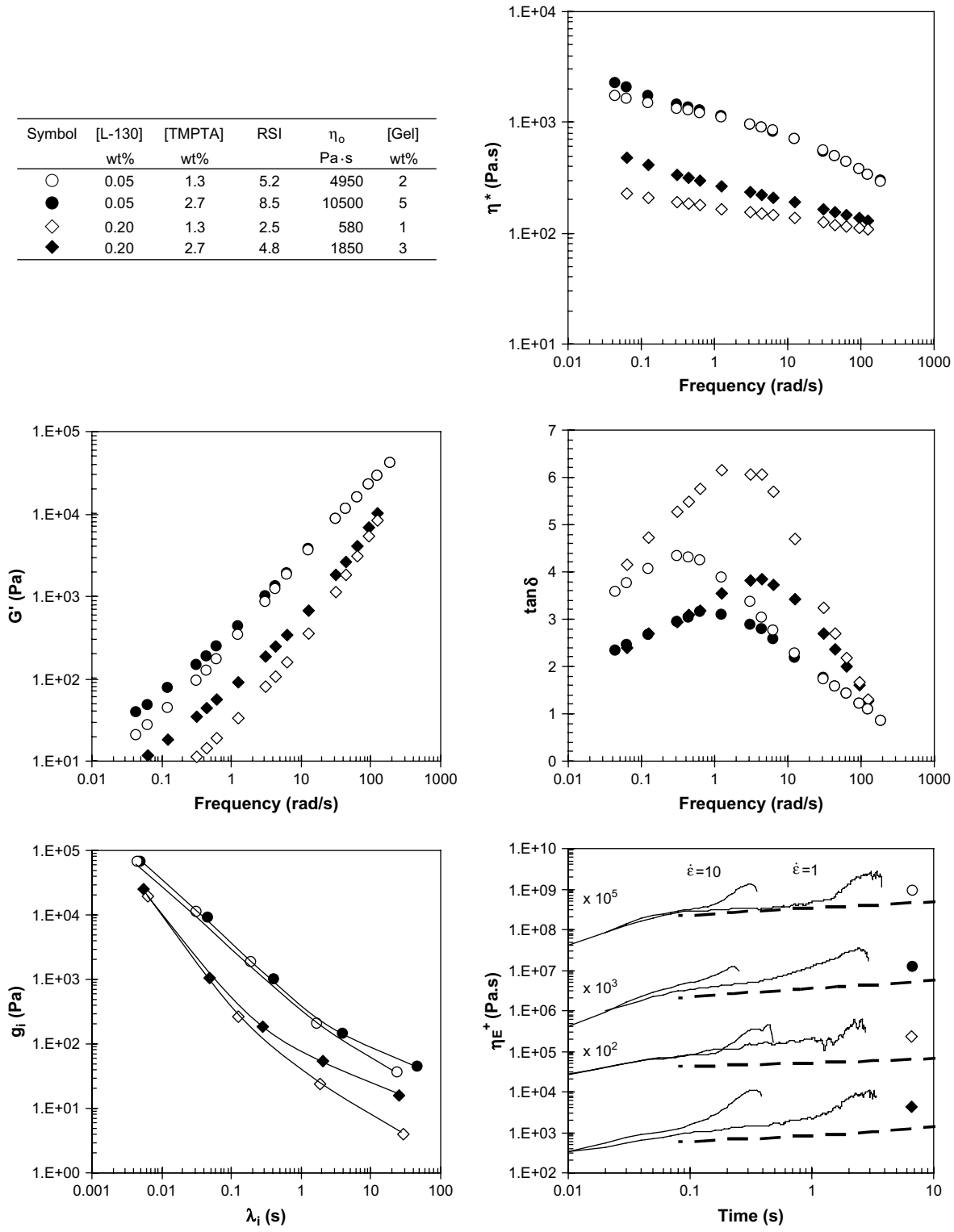

Fig. 5. Rheological data for PP-*g*-TMPTA products ($T = 180\ ^\circ C$).

relaxation spectrum, whose RSI was shifted from 8.8 for the starting material to 39.4 for the TAP derivative. So influential was this gel fraction that a steady-state condition could not be established in a creep experiment, which prevented us from observing a meaningful zero-shear viscosity.

The range of rheological properties accessible from a coagent-grafting approach is illustrated in Fig. 7. At low initiator and coagent loadings, TMPTA generated a greater hyper-branched gel population than did TAP, resulting in higher low-frequency viscosity (Fig. 7a). However, very similar gel contents and rheological properties were observed when 0.05 wt% of L-130 was used to activate 90 μmol/g of each coagent (Fig. 7b). This coincidence is remarkable, given the differences in kinetic reactivity and cross-linking potential of TMPTA and TAP. Under these particular reaction conditions, both coagents gave architectures that were indistinguishable by dynamic rheological analysis.

Symbol	[L-130]	[TAP]	RSI	η_o	[Gel]
	wt%	wt%		Pa·s	wt%
○	0.05	1.0	2.8	1260	1
●	0.05	2.0	12.2	5540	4
◇	0.20	1.0	2.1	240	<1
◆	0.20	2.0	39.4	N/A	9

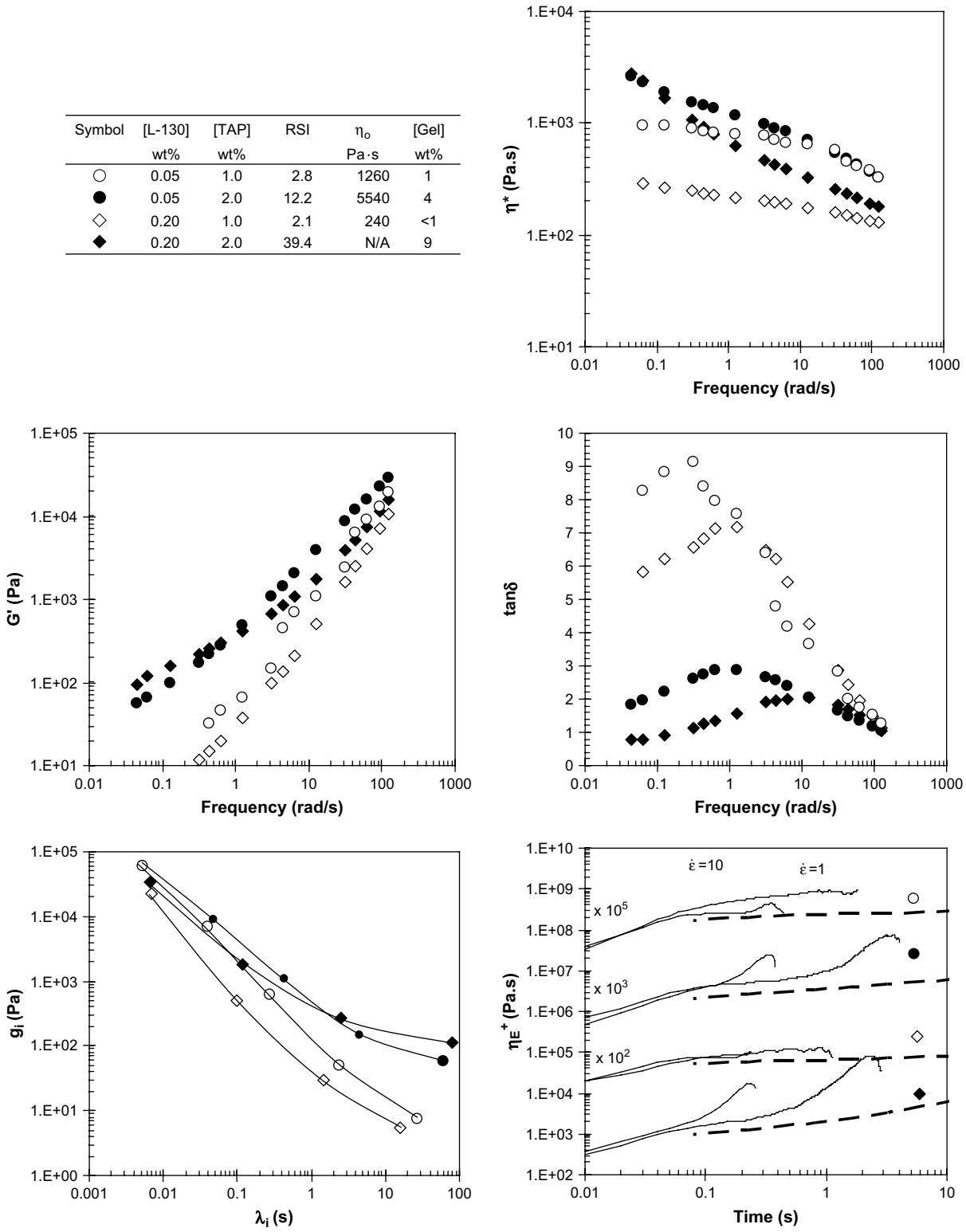

Fig. 6. Rheological data for PP-*g*-TAP Products ($T = 180\ ^\circ C$).

This coincidence was lost on moving to higher initiator loadings (Fig. 7c). Using 0.20 wt% of peroxide, TAP generated 9 wt% of gel, compared with just 3 wt% in the analogous PP-*g*-TMPTA material. This difference resulted in elevated low-frequency viscosities for the TAP system, while high-frequency properties diverged to a lesser extent, since they are dominated by the low molecular weight sample matrix.

6. Discussion

The synthetic approach explored in this work transforms the architecture of PP through a balance of crosslinking and chain scission. PP macro-radicals (P•) are needed to support coagent addition, since grafting proceeds by an initial attack on the C═C bond of a coagent, as follows.

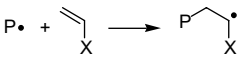

In most cases the resulting adduct radical is not susceptible to fragmentation, meaning that a coagent can serve in a molecular weight stabilizing role [5]. However, hydrogen atom transfer from PP to the intermediate adduct is needed to sustain the chain character of coagent-assisted crosslinking.

Only through this closed reaction sequence can multiple C=C additions be achieved for each radical introduced by the initiator. As a result, unless all chain character is sacrificed, a finite PP macro-radical population is inevitable. This is important, since it is the unimolecular fragmentation of tertiary PP macro-radicals that leads to molecular weight loss. Since finite PP macro-radical concentrations are the inevitable consequence of an efficient coagent-grafting process, a degree of polymer scission is also inevitable.

The reactivity of a coagent with respect to the radical addition and hydrogen transfer reactions illustrated above dictates the kinetic chain length (KCL) of PP crosslinking. A high KCL coagent will reach full C=C conversion, and hence generate its maximum crosslink density, using relatively few macro-radicals. Initiator loadings can be lowered in these cases, and the extent of PP fragmentation can be reduced without affecting crosslink yields. As a result, a high KCL coagent can support a different crosslinking versus scission balance than a less reactive analogue.

Equally important to overall crosslinking and fragmentation yields is the distribution of crosslinks and scission products amongst polymer chains. As described above, a coagent-based approach to PP branching is inclined to produce bimodal products. Radical activity is disproportionately intense amongst the largest chains of the molecular weight distribution. At first glance, this would not appear to be problematic, as both chain scission and coagent addition would exhibit the same molecular weight bias. However, coagent grafting produces functionalized chains that are far more reactive with respect to molecular weight growth, and the resulting branched architecture is much less susceptible to molecular weight loss by chain scission. Conversely, scission of ungrafted, linear chains produces low mass fragments that are less susceptible to molecular weight growth by coagent-assisted crosslinking.

These arguments suggest that bimodality is an inherent feature of coagent-based PP modifications. Products are comprised of a degraded "matrix" material and hyper-branched material whose molecular weight can be extended beyond the gel point. The amount and molecular weight of each chain population is a function of coagent reactivity, the amount of peroxide employed, and the reaction temperature. Scheme 2 illustrates a simplified representation of the first two variables. In general, the molecular weight of the majority chain population, denoted as "Matrix M_n" declines as peroxide loadings are raised. On the other hand, crosslink densities will increase as long as residual C=C functionality remains in the system. Since a reactive coagent such as TMPTA requires relatively low peroxide loadings, it can produce hyper-branched material while incurring a minimal amount of matrix degradation. Its primary deficiency centres on its propensity toward homopolymerization, which reduces overall crosslinking efficiency. A more efficient, but less reactive, coagent such as TAP requires higher peroxide loadings to generate a given network density, and will therefore be accompanied by lower matrix molecular weights.

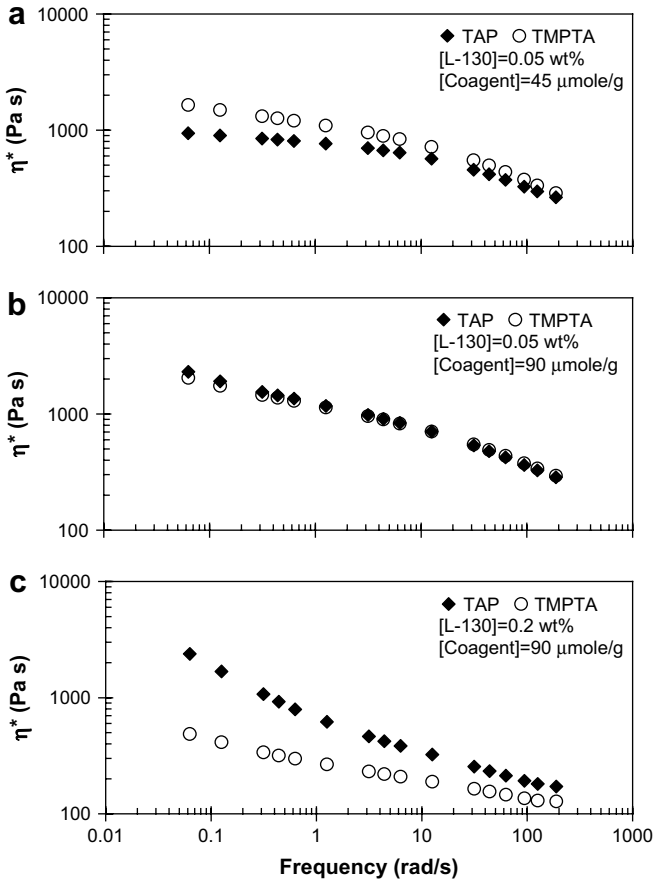

Fig. 7. Comparison of PP-*g*-TAP and PP-*g*-TMPTA product rheology.

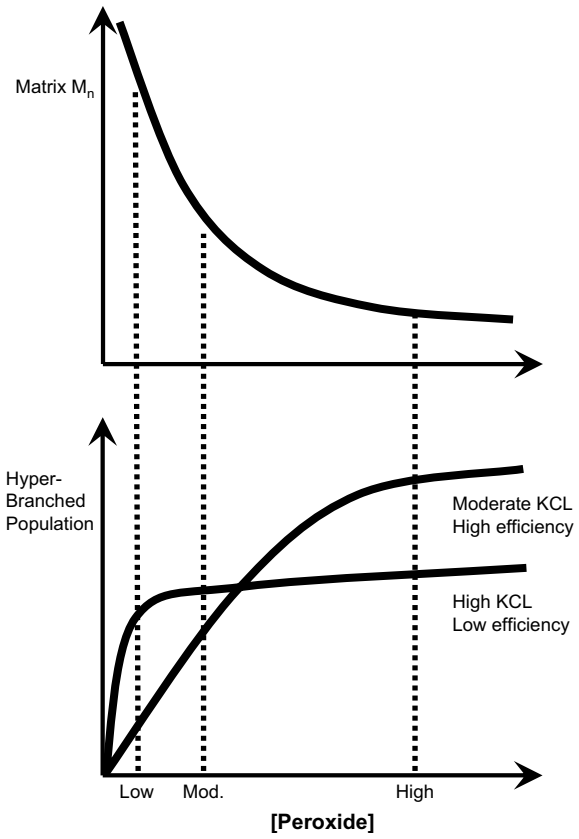

Scheme 2. Simplified illustration of PP-*g*-coagent structure development.

In closing, we note that the simultaneous grafting of coagents and functional monomers such as maleic anhydride has

attracted recent attention [25,26]. Under these circumstances, initiator loadings should be governed by the least reactive C=C bond. If high peroxide concentrations are needed to achieve the desired functional monomer conversion, then the kinetic reactivity of a coagent is of less concern than its crosslinking efficiency.

7. Conclusions

The coagent-based approach to PP branching generates bimodal products comprised of a degraded, lightly branched matrix and a relatively small amount of hyper-branched material. Melt elasticity and extensional properties are enhanced in the cases where the molecular weight of hyper-branched polymer exceeds the gel point. Therefore, careful consideration of the kinetic reactivity and crosslinking efficiency of a given PP-coagent pair can generate a wide range of branched architectures and rheological properties.

References

[1] Gotsis AD, Zeevenhoven BLF, Tsenoglou C. J Rheol 2004;48:895–914.
[2] Auhl D, Stange J, Munstedt H, Krause B, Voigt D, Lederer A, Lappan U, Lunkwitz K. Macromolecules 2004;37:9465–72.
[3] Janzen J, Colby RH. J Mol Struct 1999;485–486:569–84.
[4] Graebling D. Macromolecules 2002;35:4602–10.
[5] Romani F, Corrieri R, Braga V, Ciardelli F. Polymer 2002;43:1115–31.
[6] Langston JA, Colby RH, Chung TCM, Shimizu F, Suzuki T, Aoki M. Macromolecules 2007;40:2712–20.
[7] Kim BK, Kim KJ. Adv Polym Technol 1993;12:263–9.
[8] Wang X, Tzoganakis C, Rempel GL. J Appl Polym Sci 1996;61:1395–404.
[9] Wang XC. PhD thesis, University of Waterloo; 1996.
[10] Nam GJ, Yoo JH, Lee JW. J Appl Polym Sci 2005;96:1793–800.
[11] Borsig E, van Duin M, Gotsis AD, Picchioni F. Eur Polym J 2008;44:200–12.
[12] Parent JS, Sengupta SS, Kaufman M, Chaudhary BI. Polymer 2008;49:3884–91.
[13] Baumgaertel M, Winter HH. Rheol Acta 1989;28:511–9.
[14] Wasserman SH. Proceedings of the 55th annual technical conference – Society of Plastics Engineers, vol. 1; 1997. p. 1129–33.
[15] Leal V, Lafuente P, Alicante R, Perez R, Santamaria A. Macromol Mater Eng 2006;291:670–6.
[16] Parent JS, Cirtwill S, Penciu A, Whitney RA, Jackson P. Polymer 2003;44:953–61.
[17] Ratzch M, Zschach T. Plaste und Kautschuk 1974;21:245.
[18] Ragharan PVT, Nandi US. J Polym Sci 1970;A-1(8):3079.
[19] Won Shing JB, Baker WE, Russell KE. J Polym Sci Part A Polym Chem 1995;33:633–42.
[20] Bartlett PD, Altschul R. J Am Chem Soc 1945;67:816–22.
[21] Tzoganakis C, Vlachopoulos J, Hamielec AE. Polym Eng Sci 1989;29:390–6.
[22] Ryu SH, Gogos CG, Xanthos M. Adv Polym Technol 1992;11:121–31.
[23] Trinkle S, Friedrich C. Rheol Acta 2001;40:322–8.
[24] Trinkle S, Walter P, Friedrich C. Rheol Acta 2002;41:103–13.
[25] Zhang L, Guo B, Zhang Z. Gaodeng Xuexiao Huaxue Xuebao 2001;22:1406–9.
[26] Sengupta SS, Parent JS, McLean JK. J Polym Sci Part A Polym Chem 2005;43:4882–3.